2010-03

Friction Stir Processing (FSP) of As-Cast AA5083 for Grain Refinement and Superplasticity

Hayashi, J.T.; Menon, S.K.; Suc, J.-Q.; McNelley, T.R.

Elsevier

Hayashi, J. T., et al. "Friction stir processing (FSP) of as-Cast AA5083 for grain refinement and superplasticity." Key Engineering Materials. Vol. 433. Trans Tech Publications Ltd, 2010.
http://hdl.handle.net/10945/66763

Key Engineering Materials
ISSN: 1662-9795, Vol. 433, pp 135-140
doi:10.4028/www.scientific.net/KEM.433.135

Online: 2010-03-29

Friction Stir Processing (FSP) of As-Cast AA5083 for Grain Refinement and Superplasticity

J.T. Hayashi[a], S.K. Menon[b], J.-Q. Su[c] and T.R. McNelley[d]

Department of Mechanical and Astronautical Engineering, Naval Postgraduate School, Monterey, CA 93943-5146 • USA

[a]jthayashi@nps.edu, [b]skmeno1@nps.edu, [c]jsu@nps.edu, [d]tmcnelley@nps.edu

Keywords: Friction stir processing; AA5083; Continuous casting; Grain refinement; Superplasticity.

Abstract. Multi-pass FSP was conducted on continuously-cast (CC) AA5083 materials in the as-cast condition. Stir zone grains were refined to ~1.0 – 3.5μm in size and highly superplastic response was obtained during tension testing of the as-processed materials at 450°C (>1200 pct. elongation at 10^{-1} s^{-1}). Current models of recrystallization do not predict adequately the highly refined grains and predominantly random textures that are observed in stir zones. Grain refinement during FSP is accompanied by refinement and redistribution of non-deforming constituents in the absence of particle fracture. The mechanics of the homogenization process remain to be established and requirements for redistribution mechanisms will be summarized. Comparison reveals that results from FSP of the as-cast material are superior to those attained in conventional processing.

Introduction

Various friction stir technologies have been developed based on the concept of friction stir welding (FSW), which was invented at The Welding Institute in 1991 as a solid-state joining method for use with aluminum alloys [1]. Thus, FSP is an extension of FSW and recent reviews have provided detailed descriptions of this and related processing and joining methods [e.g., 2-4]. Briefly, during FSP a non-consumable rotating tool consisting of a cylindrical shoulder and a projecting concentric pin is pressed into the surface of the work piece. Initially, friction between the pin and work piece softens the material and, subsequently, a combination of frictional and adiabatic heating results in the formation of a plasticized column of metal (the stir zone) surrounding the tool pin. Once the tool shoulder comes in contact with the work piece surface the tool is traversed in a pre-determined pattern to process a volume of material defined by the processing pattern and tool pin length. Processing parameters for FSP include the step-over distance between successive passes. This distance must be small enough to assure overlap of the stir zones formed in successive passes in order to achieve uniform deformation throughout the processed region.

AA5083 is widely used for marine, aerospace and other transportation applications. Quick plastic forming (QPF) of automobile body components has used direct-chill (DC) cast material that has been processed by hot and warm rolling to a hot band condition and then cold worked an H-19 temper prior to QPF [5]. In this application, a recrystallized grain size of 7 - 8μm provides sufficient ductility to support hot blow forming at 450°C [6-9]. The substitution of CC material would provide cost savings but CC material typically exhibits poorer ductility at 450°C due to less straining during prior hot working to produce the hot band condition [6].

In the present investigation, FSP has been applied to continuously cast (CC) AA5083 in the as-cast condition in order to assess the potential for grain refinement by the thermomechanical cycle of this process. Other applications of FSP to cast materials have included processing of cast NiAl bronze to enhance strength and ductility of the surface layers of large marine castings [10-12], and

FSP of investment-cast Ti-6Al-4V to refine microstructure and enhance strength and fatigue resistance [13]. In such applications FSP is intended to convert the as-cast microstructure to a wrought condition in the absence of macroscopic shape change, and highly refined grain sizes have been reported in such investigations. Indeed, superplastic ductility exceeding that in conventionally processed CC AA5083 has been achieved by FSP of an Al-Mg-Zr alloy [14]. Here, two different combinations of tool and processing parameters have been employed and grain refinement as well as superplastic response has been evaluated.

Experimental Procedures

Material. As-cast CC AA5083 material was provided in the form of 15mm thick plates and composition data are provided in Table 1.

Table 1. Composition Data [wt. pct.] for the CC AA5083 Material

Material	Mg	Mn	Si	Fe	Cr	Cu	Al
CC-G1	4.70	0.72	0.07	0.22	-	0.02	Bal.

This material has been the subject of previous reports wherein a maximum ductility of ~200pct. elongation was obtained at 450°C and strain rates of 5×10^{-4} - $5\times10^{-2}s^{-1}$ in conventionally processed material. The conventional production route involves direct rolling of the as-cast material to a hot band thickness of 4 – 5mm followed by cold rolling to a reduction of ~74pct. to provide sheet 1.2mm in thickness having an –H19 temper.

FSP of As-cast CC AA5083. The FSP was conducted using two different tool designs and processing conditions. The tools were both fabricated in H-13 steel that was heat treated to HRC52. Table 2 summarizes the two FSP runs for the results of the current investigation.

Table 2. FSP Tools and Processing Conditions

Run	Pin Features	Pin Dimensions, [mm]	FSP Parameters			
			RPM	Traversing Rate [mm/min]	Pass Sequence	Step Over, [mm]
1	Threaded and tapered,3° cone angle	18 (shoulder dia.) 5 (length) 6 (base dia.) 4 (tip dia.)	350	101.6	5 parallel passes	2
2	Threaded and straight, 3° cone angle	9(shoulder dia.) 3(length)	800	90	3 parallel passes	2

Microstructure Analysis. Samples for optical microscopy were polished through a 0.5μm diamond suspension and examined using bright field illumination in a Nikon Epiphot 200 inverted microscope after etching in a 10pct. H_3PO_4 solution heated to 50°C. Backscatter electron (BSE) imaging and orientation imaging microscopy (OIM) characterization required a final elecropolishing step using a solution of 80pct. ethanol, 6pct. H_3ClO_4 acid and 14pct. H_2O for 20s at 15V. Observations were conducted in a Zeiss Neon40 FE-SEM + FIB operating at 20KV. One sample was examined in STEM mode after final thinning by FIB in this microscope.

Mechanical Testing. Tension testing was conducted at 450°C at constant nominal strain rates ranging from 3×10^{-4} to $3\times10^{-1}s^{-1}$ using sheet-type samples having gage sections 8mm in length, 2mm in width, 1mm in thickness and with a radius of 1.6mm at the shoulder. The samples were obtained by wire electric discharge machining (EDM) from the stir zones after completion of the FSP. The samples were always lightly ground on all surfaces to remove any damage layer formed during EDM. The testing utilized and Instron Model 4507 load frame equipped with either a 500N or 10,000N load cell. Each tension test was conducted to failure at a constant extension rate after heating and equilibration at the test temperature for approximately 20mins. Temperature control was accomplished using a five-zone clamshell furnace mounted on the load frame.

Results and Discussion

Transverse sections showing the stir zones and surrounding base metal of the two FSP runs are shown in Fig. 1. The interface between the stir zone and base metal is more distinct on the advancing side (tangential speed of the tool surface adds to the traversing speed) than on the retreating side (tangential speed of the tool surface subtracts from the traversing speed), as well as a tunnel defect is apparent on the lower advancing side in run 1. This defect was eliminated in run 2.

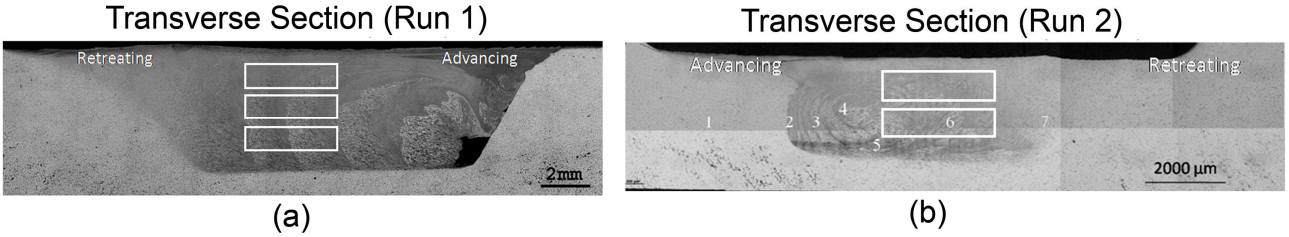

Fig. 1. Transverse sections through the stir zones of (a) run 1 material processed at 350rpm and 101.6mm min-1and (b) run 2 material processed at 800rpm and 90mm min^{-1}

The outlines of the tensile sample gage sections are illustrated by the white rectangles; three samples were obtained from the depth of the stir zone in run 1 while only two could be obtained from run 1.

Non-equilibrium solidification in the base metal is evident in Fig. 2a while a refined and homogeneous distribution of constituent particles is apparent in the stir zone, Fig. 2b, for material processed in run 1. Similar results were obtained in run 2. At the resolution of the optical

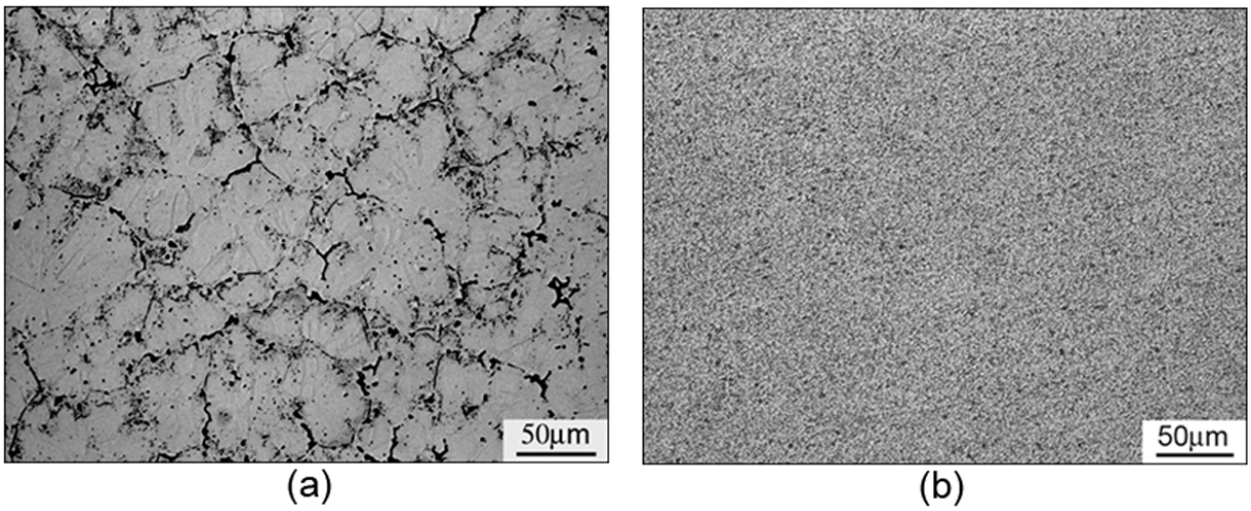

Fig. 2. Optical microscopy from the base metal ,(a) , and stir zone, (b), of the CC AA5083 processed in run 1at 350rpm and 101.6mm min-1, illustrating homogenization of the structure.

micrographs in Fig. 2, FSP has both refined as well as redistributed the coarse dark-etching Al_6Mn phase in the absence of damage in the form of particle cracking or porosity in the matrix. Fig. 3a shows the microstructure of the stir zone at higher resolution in a BSE image for the material of run 2; the Al_6Mn phase (light in contrast) is distributed uniformly in the microstructure as particles 0.1 – 2.0µm in size while the $\beta(Al_8Mg_5)$ is located along grain boundaries as particles 0.2 – 0.5µm in size. From contrast variation in Fig. 3a the grain size is ~2µm. Refined particles as fine as 20nm in size are apparent in the STEM image for this same material shown in Fig. 3b. Grain size determination by OIM methods is presented in Fig. 4 for both runs 1 and 2. The mean linear intercept grain sizes are 0.95µm (area weighted grain size of 1.9µm) for material processes at the lower rpm in run 1 and

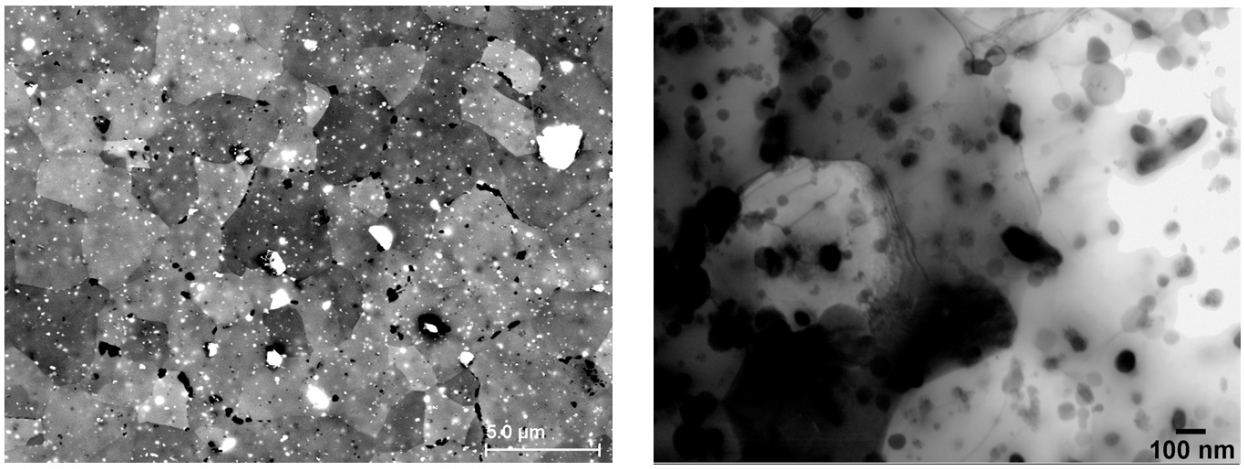

Fig. 3. Backscatter electron image from the stir zone of the CC AA5083 processed in run 2 at 800rpm and 90 mm min-1, (a), showing homogeneous and refined constituents; a STEM image of this region , (b), shows refined constituent particles 10 - 50nm in size.

1.75µm (area weighted grain size of 3.5µm) for material processed at a higher rpm in run 2. These values are 5 – 10 × finer than attained in conventional processing. The particle stimulated nucleation (PSN) model [15] for recyrstalliztion adequately predicts the grain sizes and random textures in AA5083 materials processed by conventional rolling practice and recrystallized during heating at 450°C. The PSN model requires the presence of non-deforming particles of minimum size $d_{particle,f} \geq 2\mu m$ in order to support the formation of deformation zones in which nuclei for new grains can form during the thermomechanical cycle of FSP [16]. Then,

$$d \approx \frac{d_{particle,f}}{1.25V_f^{1/3}} \tag{1}$$

where d is the grain size and V_f is the volume fraction of nucleating particles. Eq. 1 suggests that $V_f \rightarrow 1.0$ to account for grains approaching 1.0µm in size. Thus, there are not enough particles of sufficient size in the microstructure to predict such refinement and alternative models of refinement are needed.

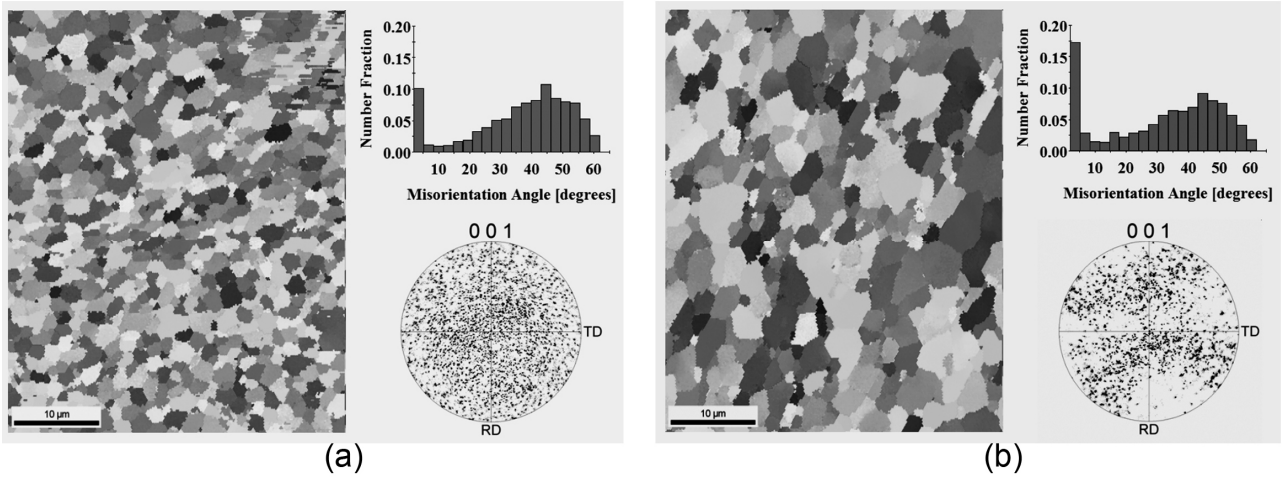

Fig. 4. OIM grain maps from the stir zones of (a) run 1 material processed at 350rpm and 101.6mm min-1and (b) run 2 material processed at 800rpm and 90mm min-1 illustrating refinement to a mean linear intercept grain size of ~1.0µm in run 1 and ~3.5µm in run 2.

In Fig. 5, the elevated temperature mechanical behavior of the CC AA5083 materials processed by FSP is compared to that of AA5083 produced by either DC or CC methods followed by conventional rolling practice. Fig. 5a shows plots of the flow stress at a strain of 0.1, $\sigma_{0.1}$, as a function of the strain rate, $\dot{\varepsilon}$, while Fig. 5b contains plots the ductility as percent elongation to failure as a function of $\dot{\varepsilon}$. Examination of these data demonstrates that the FSP materials exhibit lower flow stresses as well as larger strain rate sensitivity coefficients, $m \equiv \partial \log \sigma / \partial \log \dot{\varepsilon}$. Furthermore, the run 1 material, with an as-processed grain size of 0.95μm, exhibits a lower in flow stress and larger *m* value than the run 2 material, which has an as-processed grain size of 3.5μm. For

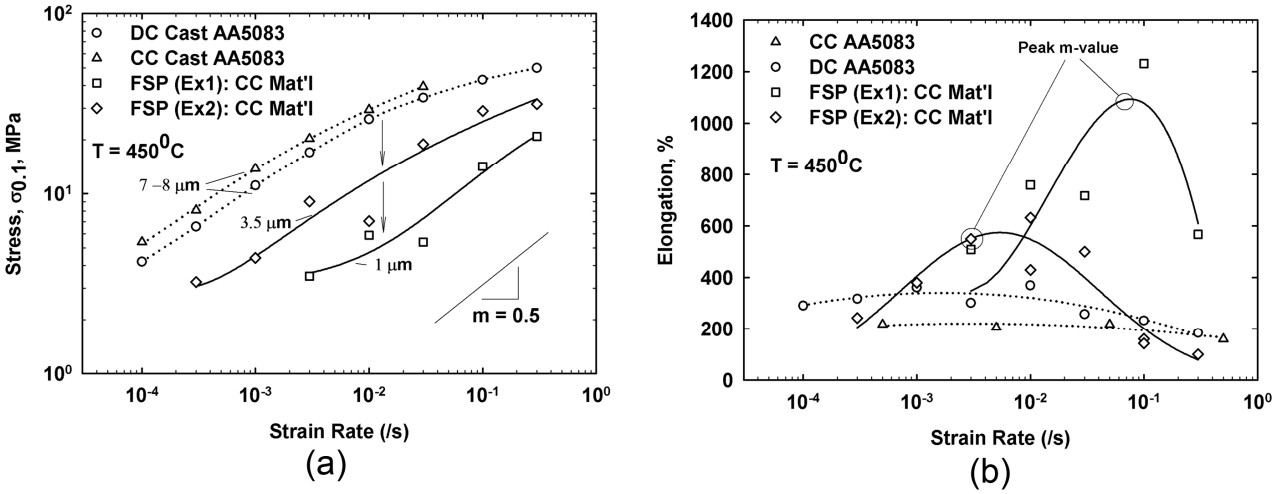

Fig. 5. Graphs of flow stress as a function of strain rate, (a), and ductility as a function of strain rate, (b), comparing runs 1 and 2 to data for conventionally processed AA5083.

these AA5083 materials the relationship among flow stress, strain rate and grain size during deformation at 450°C is given by [9]

$$\dot{\varepsilon}_{total} = A_1 \frac{D^*_{eff}}{d^2}\left(\frac{\sigma}{E}\right)^2 + A_2 D_{solute}\left(\frac{\sigma}{E}\right)^{n_{sdc}} \tag{2}$$

where $\dot{\varepsilon}_{total}$ is the strain rate, A_1 is a material constant, D^*_{eff} is the effective diffusion coefficient, *d* is the grain size, σ is the flow stress, *E* is Young's modulus, A_2 is also a material constant, D_{solute} is the solute diffusion coefficient (for Mg in Al), and $n_{sdc} \approx 4$ is the stress exponent for solute drag creep (SDC). The first term on the right in Eq. 1 describes the contribution of grain boundary sliding (GBS), with a stress exponent $n = 2$, to the total deformation rate while the second term on the right in this equation is the SDC contribution. According to Eq. 1, when GBS predominates during deformation the strain rate sensitivity $m \to 0.5$ and the flow stress will be proportional to the grain size. Indeed, examination of all four plots in Fig. 5a shows that the finer grain sizes of the FSP materials leads to progressively and proportionally lower flow stress values for $\dot{\varepsilon} \le 10^{-2}$ s^{-1}. These finer grain sizes also increase the strain rate range for GBS control of deformation and this is reflected in the occurrence of peak ductility at higher values of strain rate, i.e., $\dot{\varepsilon} \to 10^{-1}$ s^{-1} for the run 1 material. Dynamic grain growth, which may account for decreased *m* value as strain rate decreases, and thus lower ductility, will be the subject of future investigations. Also, cavity formation and growth in the FSP materials will also be the subject of a subsequent report.

Conclusions

The following conclusions may be drawn from this investigation.

1. FSP may be employed to convert an as-cast microstructure to a wrought condition in the absence of macroscopic shape change.

2. The grain size of CC AA5083 material may be refined to ~1.0μm in size within the stir zone; improved models for grain refinement are required in order to account for such refined grains during FSP
3. Both soluble and insoluble constituents of microstructure can be refined in size and redistributed by FSP to produce homogeneous particle distributions in the absence of microstructure damage.
4. Superplastic ductility exceeding 1000pct. elongation to failure at a strain rate of $10^{-1}s^{-1}$ and 450°C was attained after FSP of CC AA5083.

Acknowledgement

The authors acknowledge financial support for this research from the University of Texas – Austin (Prof. Eric Taleff) and General Motors Corporation (Dr Paul Krajewski) as well as partial support from the Office of Naval Research (Contract No. N00014-06-WR-2-0196, Dr Julie Christodoulos).

References

[1] W.M. Thomas, et al.: G.B. Patent 9125978.8 (1991)

[2] R.S. Mishra and M.W. Mahoney (eds.): *Friction Stir Welding and Processing* (ASMI, Materials Park, OH, 2007)

[3] R.S. Mishra and Z.Y. Ma: Mater. Sci. Eng. R, vol. 50 (2005), p. 1

[4] R. Nandan, T. DebRoy and H. K. D. H. Bhadeshia: Prog. Mater. Sci., vol. 53 (2008), p. 980

[5] J.G. Shroth: in *Advances in Superplasticity and Superplastic Forming*, edited by E.M. Taleff, et al., TMS, Warrendale, PA (2004), p. 9

[6] M.A. Kulas, et al.: Metall. Mater. Trans. A, vol. 36A (2005), p. 1249

[7] E.M. Taleff, et al.: Mater. Sci. Eng. A, vols. 410-11 (2005), p. 32

[8] M.A. Kulas, et al.: Metall. Mater. Trans. A, vol. 37A (2006), p. 645

[8] W.P. Green, et al.: Metall. Mater. Trans. A, vol. 37A (2006), p. 2727

[9] T.R. McNelley, et al.: Metall. Mater. Trans. A, vol. 39A (2008), p. 50

[10] K. Oh-Ishi and T.R. McNelley: Metall. Mater. Trans. A, vol. 35A (2004), p. 2951

[11] K. Oh-Ishi and T.R. McNelley: Metall. Mater. Trans. A, vol. 36A (2005), p. 1575

[12] K. Oh-Ishi, A.P. Zhilyaev and T.R. McNelley: Metall. Mater. Trans. A, vol. 37A (2006), p. 2239

[13] A.L. Pilchak, M.C. Juhas and J.C. Williams: Metall. Mater. Trans. A, vol. 38A (2007), p. 401

[14] Z. Y. Ma and R. S. Mishra: Scripta Materialia, 53 (2005), p. 75

[15] F.J. Humphreys and M. Hatherly: *Recrystallization and Related Annealing Phenomena* (Elsevier, Oxford, 2004)

[16] T.R. McNelley, S. Swaminathan and J.Q. Su: Scripta Mater., vol. 58 (2008) p. 349